Numerical Heat Transfer, Part A, 35:797–814, 1999

1040–7782/99 $12.00 + .00

NUMERICAL STUDY OF HEAT TRANSFER IN TWO-ROW HEAT EXCHANGERS HAVING EXTENDED FIN SURFACES

Tony W. H. Sheui, S. F. Tsai, and T. P. Chiang
Department of Naval Architecture and Ocean Engineering, National Taiwan University, 73 Chou-Shan Road, Taipei, Taiwan, Republic of China

This paper reports on a three-dimensional study of air through two-row cylinder tubes. The analysis is intended to present a comparison of numerical and experimental data to validate the laminar flow postulation. The current study explores the influence of four perforated fin surfaces on the pressure drop and heat transfer rate. To gain further insight into the three-dimensional vortical flow structure, we conduct a topological study of the velocity field. Examination of the surface flow topology and the flow patterns at cross-flow planes sheds some light on the complex interaction of the cylinder tube with the mainstream flow. This study clearly reveals a saddle point in front of the first row of cylinder tubes. Also clearly revealed by the computed solutions is a flow reversal found in the wake of the tube. The character of the critical-point-induced flow is also addressed. This study shows that the addition of perforated fins is not without deficiency. There is, in fact, a trade-off between the benefit of having an improved heat transfer and the penalty of having an increased pressure drop.

INTRODUCTION

The present study was undertaken in order to gain a more comprehensive understanding of the effect of fin types used in conjugate heat exchangers on the heat transfer between the gas and the fin. Among fins, which can be classified mainly as plain, corrugated, punched, and slotted types, slotted fins have received considerable attention and seen increasing use. The main reason slotted fins can provide heat transfer enhancement is the secondary flow formation, which aids mixing of flow in the transverse plane. The other important factor is the repeated formation-destruction of the thin boundary layer flow.

Among the various fins in existence, we consider slotted fins because of their wider popularity. Slotted fins can be divided into louvered, Forgo, radial-strip, parallel-strip, and wavy-strip types. Among these, wavy- and parallel-strip fins are probably the most attractive. The flow pattern is considered to be complex even in the geometrically simplest plate-fin heat exchanger. The physical complexity comes from the three-dimensional boundary layer development and the subsequent flow separation. The introduction of slotted fins adds further complications. Experimen-

Received 13 September 1998; accepted 2 December 1998.
Financial support was made available by the Teco Electric & Machinery Co. Ltd. We are glad to have this opportunity to acknowledge this support and to record our thanks.
Address correspondence to Professor Tony W. H. Sheu, Institute of Naval Architecture, National Taiwan University, 73 Chou-Shan Road, Taipei Taiwan, Republic of China.

NOMENCLATURE

A	maximum flow area of a cell, m^2	$\overline{P}$	span-averaged pressure, Pa
A_c	minimum flow area in a cell, m^2	$\dot{q}$	heat flux, W/m^2
A_f	transfer area of a cell, m^2	$\dot{q}_p$	span-averaged heat flux, W/m^2
B	tube pitch, m	Re	Reynolds number
c_p	specific heat of the air, J/(kg K)	T	temperature, K
D	tube diameter, m	u_i	velocity component along i direction, m/s
D_h	hydraulic diameter, m		
H	spacing between two plates, m	U	inlet velocity of the air, m/s
k	thermal conductivity, W/(m K)	α	thermal diffusivity ($= k/\rho c_p$), m^2/s
L	streamwise length of the channel, m	ΔP	pressure drop, Pa
$\dot{m}$	flow rate of the air, kg/s	ΔQ	span-averaged heat transfer rate, J/s
Nu	Nusselt number		
$\overline{\text{Nu}}$	span-averaged Nusselt number	ν	kinematic viscosity, m^2/s
p	pressure, Pa	ρ	density of the air, kg/m^3

tal investigation of conjugate heat transfer in regions between two fin surfaces is still a challenging task. In fact, according to Fiebig et al. [1, 2], no experimental method exists that allows measurement of heat transfer in a finned-tube element.

The alternative to experimental study is to numerically solve the governing equations for the working media. With the advent of cost-effective high-speed computers and computational models that have evolved to a high level of sophistication and reliability, it is now possible to simulate heat transfer characteristics of finned-tube heat exchangers. In the literature, only a limited number of publications focus on three-dimensional simulations of the slotted-fin heat transfer problem. The goal for the present work was to assess the performance of wavy-strip and parallel-strip type fins. This is regarded as the first step toward improvement of existing designs and thus reduction of the heat exchanger size.

The remainder of this paper is organized as follows. Working equations and the problem specifications are given in the next section. This is followed by a brief outline of the segregated solution algorithm, which was devised to compute the finite volume discretization equations in an iterative manner. To present a clear picture of the vortical flow structure, we choose limiting streamlines in our topology study. The numerical results, along with the validation study, and conclusions are presented in the remaining sections.

THEORETICAL ANALYSIS

Using a user-prescribed convective heat transfer coefficient on the fin surface, computation of heat transfer can be performed with little effort, making design of heat exchangers a practical alternative. One can also apply a more sophisticated model to obtain a detailed account of the complex physics involved in the flow passage. In order to predict essentially all possible flow and heat transfer features, we simultaneously work with the convective heat transfer problem for the working fluid and the heat conduction problem for the fin itself.

We consider here a Newtonian fluid with constant properties. The equations of motion that govern the fluid are Navier-Stokes equations and the kinematic condition that the velocity be divergence-free. The inherent nature of the problem under investigation warrants full unsteady, three-dimensional calculations that can be quite expensive. The results shown below lend credence to the assumption of steady state analysis. Numerical modeling of the flow field in Ω was thus performed under the steady and laminar assumptions:

$$\frac{\partial u_i}{\partial x_i} = 0 \tag{1}$$

$$\frac{\partial}{\partial x_m}(u_m u_i) = -\frac{1}{\rho}\frac{\partial p}{\partial x_i} + \nu\frac{\partial^2 u_i}{\partial x_m \partial x_m} \tag{2}$$

where u_i are the velocity components ($i = 1$–3) and p is the pressure. For this study, the flow under investigation was characterized by the Reynolds number, defined as $\mathrm{Re} = u_\infty H/\nu$. Here H is the spacing between two fins, while u_∞ is the inlet free-stream velocity, which enters the physical domain having a cross-sectional area of $H \times B$. The rationale behind adopting the velocity-pressure formulation is that we can solve the set of equations, Eqs. (1)–(2), with well-posed boundary conditions to determine the fluid flow and heat transfer fields.

FINITE VOLUME METHOD AND SOLUTION ALGORITHM

To conduct an analysis that is amenable to computer simulation, we begin by transforming the working equations into their algebraic counterparts. The present incompressible flow analysis was conducted on staggered grids to avoid even-odd pressure oscillations [3]. It is the velocity, which is offset by a half mesh size in its respective coordinate direction from the pressure, that adds considerable complexity to the programming.

Use of primitive variables to simulate incompressible Navier-Stokes equations may further complicate the analysis. Complications are due to the absence of pressure in the continuity equation. Not only will this absence tend to increase the condition number for the discrete system, but it will also cause more zero diagonals to occur. The resulting lack of diagonal dominance presents difficulties in the use of iterative solvers to solve for the algebraic system of equations. To overcome these difficulties, a segregated solution algorithm that is currently in widespread use is considered to be compensation for the mixed formulation. In the segregated formulation, working equations are solved in a strongly decoupled fashion. Satisfaction of the continuity equation is accomplished through increasingly improved pressure solutions. The correction of the pressure, which is governed by the Poisson equation, corresponds to incorporating the incompressibility constraint into the formulation. The storage demand for matrix equations is thus considerably reduced. Without loss of stability, this semi-implicit solution algorithm provides the same steady state solution but at much lower computational cost than does the equivalent mixed formulation.

Under conditions where grid lines are skewed to streamlines, false diffusion errors cause the prediction accuracy to deteriorate. Care must be taken; otherwise, the simulation quality may be seriously harmed by the added cross-wind diffusion errors. Deterioration of accuracy is particularly severe under high-Re circumstances. To remedy this defect, nonlinear flux terms are discretized using upwind schemes. We apply here the QUICK scheme [4] in the domain that has been nonuniformly discretized. As was the case with the elliptic problem, both diffusive fluxes and pressure gradients are approximated by means of a second-order centered scheme.

Because of geometric complexity, the study of a heat exchanger with extended fin surfaces has traditionally been a time-consuming effort, employing such techniques as coordinate transformation. However, it is now well accepted that discretization errors arising from curvilinear coordinate transformation are generally considerable and hard to resolve for problems involving highly curved grid lines. Thus, we conduct analysis here in the Cartesian coordinate system so as to predict physically realistic results with less computational effort.

PROBLEM DESCRIPTION AND BOUNDARY CONDITION

Depending on the application area, we can choose from integrating one-row or two-row cylinder tubes into the heat exchanger shown in Figure 1. Because of the lack of space, no consideration is given here to determine whether or not heat exchangers with two-row coils will outperform those with one-row coils. Our attention is simply directed toward dealing with two-row coils. A schematic illustration of the physical problem shown in Figure 2 reveals that vertical tubes of circular cross/sections are staggered with respect to each other. In the arrange-

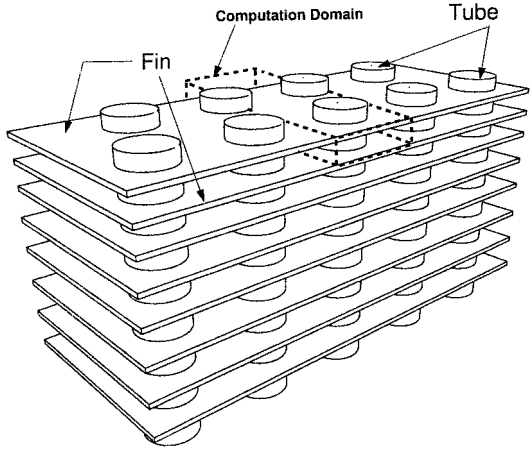

Figure 1. Schematic of two-row fin and tube heat exchanger.

ment of these tubes, the centroids of three adjacent tubes form an equilateral triangle. This fin-tube configuration is characterized by $H/D = 0.187$, $B/D = 2.72$, and $L/D = 1.693$ for a fixed value of $H = 1.4$ mm.

In this study, airflow with a free-stream velocity of u_∞ approaches the inlet plane, which is upstream of the leading edge of the fin by a distance of 4.5 mm. The proper streamwise location at which the inlet velocity profile is applied is a subject requiring further investigation and will not be addressed here. At fin surfaces where no-slip boundary conditions apply, pressure boundary condition is not permitted. In the numerical simulation of inflow-outflow problems, it is of necessity to truncate the physical domain at a synthetic outlet so as to reduce the computational expense. We prescribe here the parallel flow at the synthetic plane, which is 5 mm downstream of the trailing edge of the fin. At the outlet plane, we apply a zero temperature gradient, since this plane has been shown to be sufficiently far away from the fin surface. In order to solve the energy equation

$$\frac{\partial T}{\partial t} + \frac{\partial}{\partial x_m}(u_m T) = \alpha \frac{\partial^2 T}{\partial x_m \, \partial x_m} \tag{3}$$

we prescribe fixed temperatures at the tube surface ($T_{\text{tube}} = 323$ K) and at the inlet with $T_{\text{in}} = 300$ K. At the two vertical walls, the periodic condition is prescribed to allow analysis to be conducted in the dotted area shown in Figure 1.

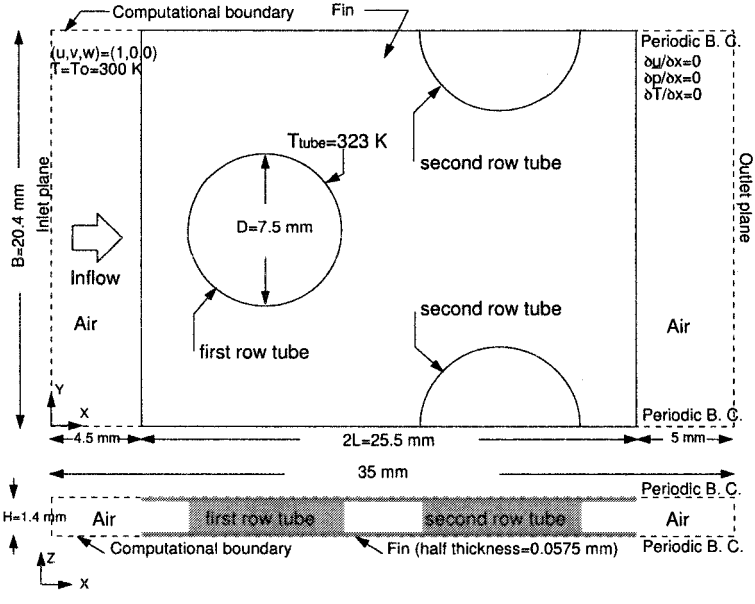

Figure 2. A finned-tube element as module geometry for the investigation. Included in this figure are also prescribed boundary conditions.

RESULTS AND DISCUSSION

As a validation study of the analysis code, we consider first a much simpler problem that involves a plate fin surface shown in Figure 1. It is the geometric simplicity that simplifies the analysis and also facilitates illustration of the flow structure. The Re under investigation is in the range of $83 \leqslant \mathrm{Re}_D \leqslant 258$, which is defined by the inlet velocities given in Figure 3. In this study, all the analyses were conducted on $142 \times 84 \times 40$ grids for the case with plate fins and on $142 \times 84 \times 54$ grids for the slotted cases. For accurately capturing the temperature and velocity boundary layers, nodal points, shown in Figure 4, are nonuniformly distributed along the x, y, z directions, respectively.

Before any computational results can be deemed reliable enough to illuminate the physical phenomenon, the computational results must be justified through the grid-independent tests. To this end, we have conducted the grid-independence study simply for the plate fin case to avoid the geometric complication. Three grids ($142 \times 84 \times 40, 82 \times 43 \times 40, 42 \times 23 \times 40$) have been attempted, from which the computed heat transfer rates are plotted in Figure 5. As this figure shows, we are led to know that grids of resolution $142 \times 84 \times 40$ are sufficient to provide

$$Re_D = \frac{\dot{m} D_h}{A_c \nu} = \frac{U D_h}{\nu} \frac{A}{A_c}$$

$\dot{m}$ = flow rate of air
D_h = hydraulic diameter
= $(4A_cL)/(A_f + \pi DH/4)$
A_c = minimum flow area in a unit cell
A_f = transfer area for a unit cell
D = tube diameter
L = streamwise length of the channel
H = spacing between plates
A = maximum flow area of a unit cell
U = inlet velocity

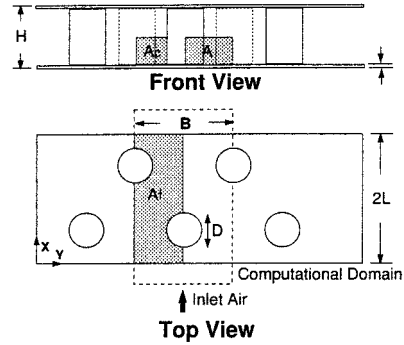

case	inlet velocity U (m/s)	Reynolds number
1	0.81	83
2*	1.00	103
3	1.20	124
4*	1.50	155
5	1.81	186
6	2.00	206

Experimental data are available

Figure 3. Definitions of Reynolds numbers and running flow conditions.

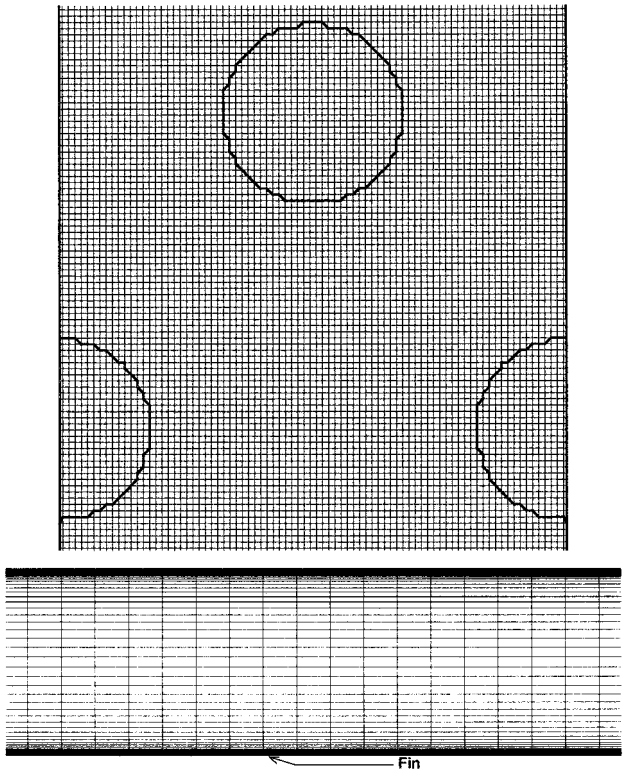

Figure 4. Grids used for the present plate fin heat transfer analysis.

grid-independent solutions both for flow and heat transfer characteristics. Figures 6 and 7 show that the experimental data agree well with the computed data in the investigated Re range, not only for the heat transfer rate, but also for the pressure drop. As Re was increased further, the deviation between the two sets of data became appreciable. We are currently trying to confirm whether this deviation is susceptible to the lack of turbulence modeling.

To gain a better understanding of flow physics and heat transfer characteristics in the conjugate heat exchanger, we have plotted limiting streamlines to show the precise surface topology. It is worth noting that the limiting streamlines shown in Figure 8 correspond to oil-streak lines in the experimental surface flow visualization [5]. In the topology study on the velocity vector field, we can obtain the critical points in the flow. Based on the eigenvalue characterization [6], we can find from Figure 8 saddle point, which is located in front of the cylinder and a wake flow pattern behind the cylinder. The location of the saddle point in the z plane is the key to determining the lines of separation on the vertical tube. We also plot in

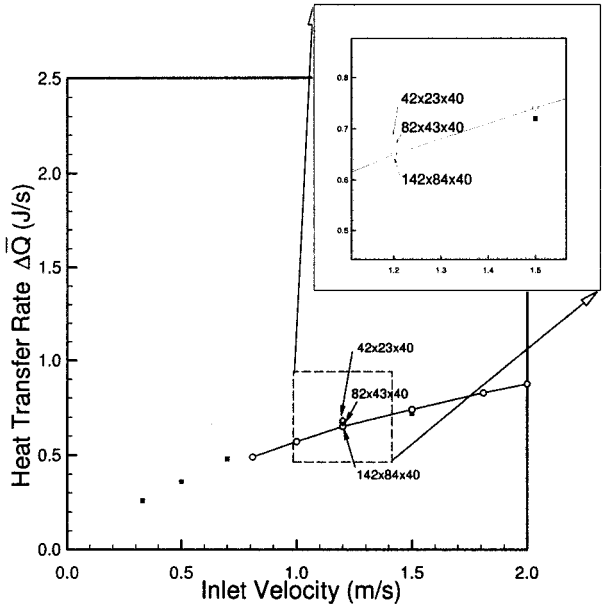

(*a*)

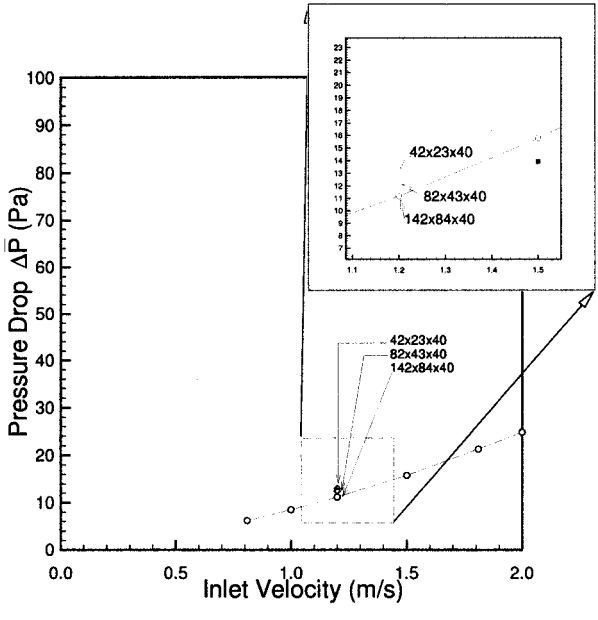

(*b*)

Figure 5. Grid-independence studies for the heat transfer analyses for the inlet velocity with 1.2 m/s. Analyses are conducted on three grids with resolutions of $142 \times 84 \times 40$, $82 \times 43 \times 40$, and $42 \times 23 \times 40$. (*a*) Heat transfer rate. (*b*) Pressure drop.

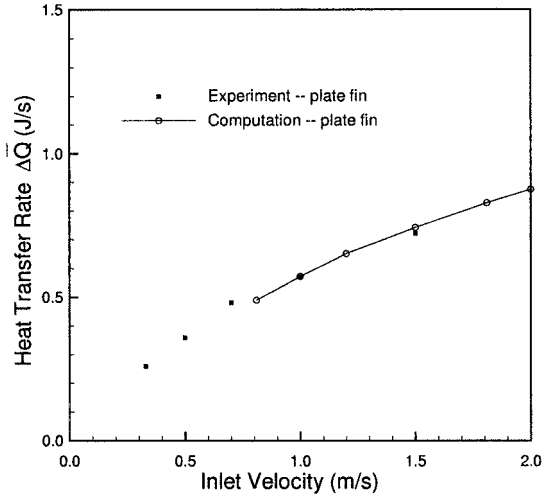

Figure 6. Comparison study of computed and measured heat transfer rate against inlet velocities summarized in Figure 3.

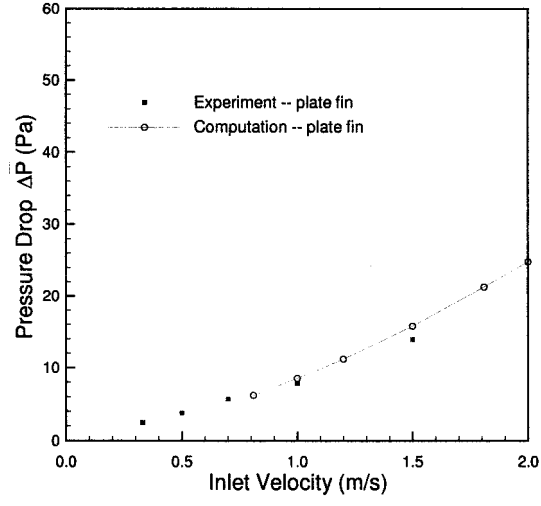

Figure 7. Comparison study of computed and measured pressure drops against inlet velocities summarized in Figure 3.

Figure 9 the three-dimensional separation and reattachment. The flow reversal seen clearly in the wake also has a great influence on the pressure drop.

In order to clearly depict the three-dimensional vortical flow structure, we plot flow lines at different cutting planes. As shown in Figure 10, critical points found at different cutting planes are integrated to form the so-called vortical core

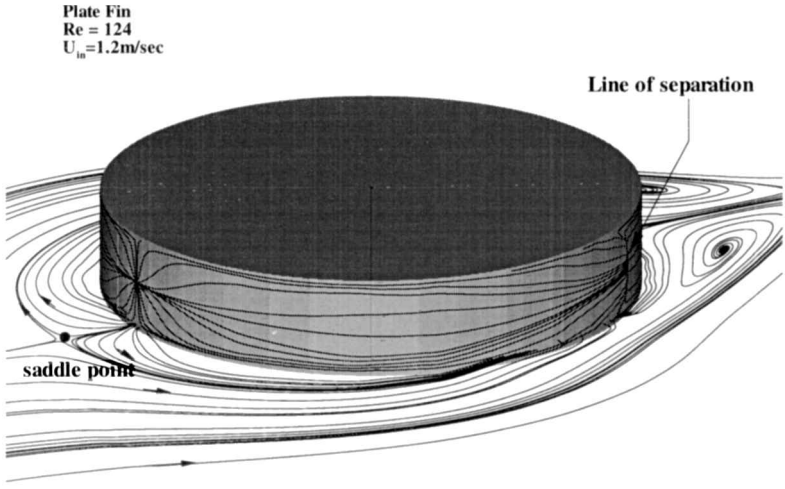

Figure 8. Limiting streamlines on the fin as well as on the tube surface.

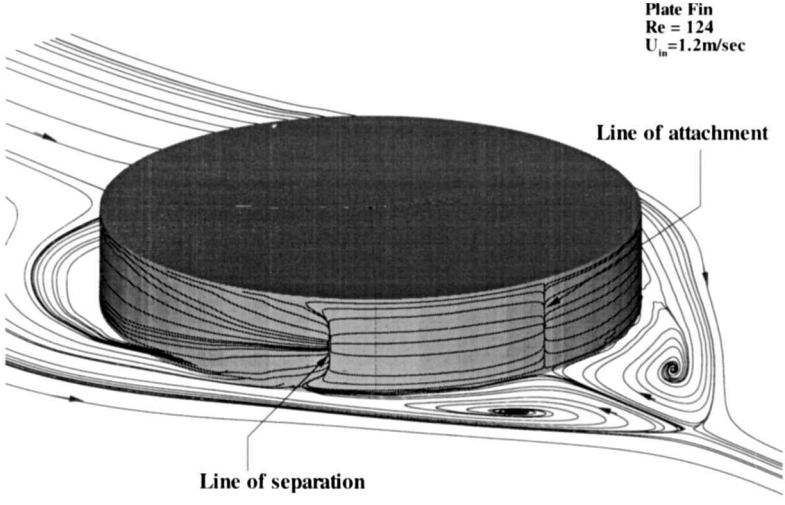

Figure 9. Illustration of lines of separation and reattachment for flows over the vertical tube.

line. The spiraling flow is found to prevail in the vicinity of the vortical core line. The spiral flow motion enhances the transfer of heat but causes the pressure drop to increase in the recirculation region, and thus more power must be consumed. It is also important to note that the size of the wake region determines the extent of heat transfer deterioration and the increase of the pressure drop. For this reason,

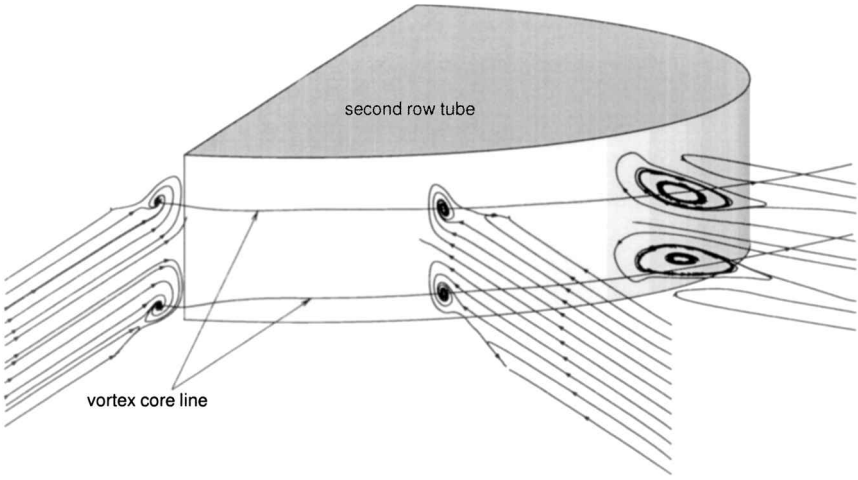

Figure 10. Illustration of the vortical core line in the flow interior.

we plot the three-dimensional wake surface in Figure 11 to show the extension of the wake into the flow regime. Figure 12 is the particle tracer plot, which produces vivid graphical illustration of spiralling motion for fluid particles in the wake.

With the analysis code verified and the flow structure for the fin-plate combination illuminated, we now turn to study geometrically and physically more complex heat transfer problems. Modeling of the subsequent problems is further complicated by the addition of irregularly shaped fins shown in Figure 13. To accurately illustrate these fin surfaces, we plot in Figures 14–16 the top view and side view of the investigated fins. To provide the necessary precision for the numerical prediction of heat transfer in a geometrically complex heat exchanger,

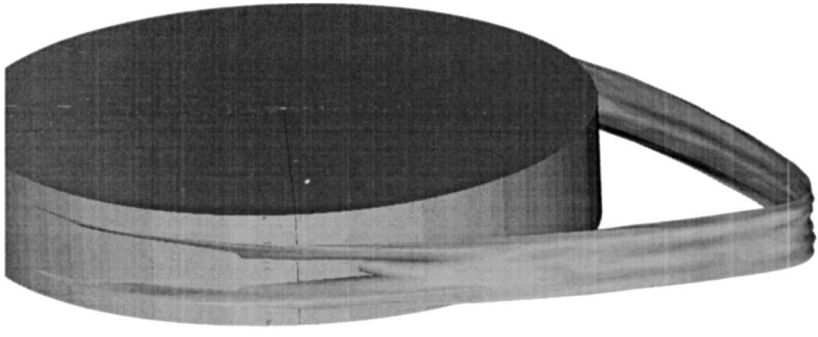

Figure 11. The computed three-dimensional wake surface.

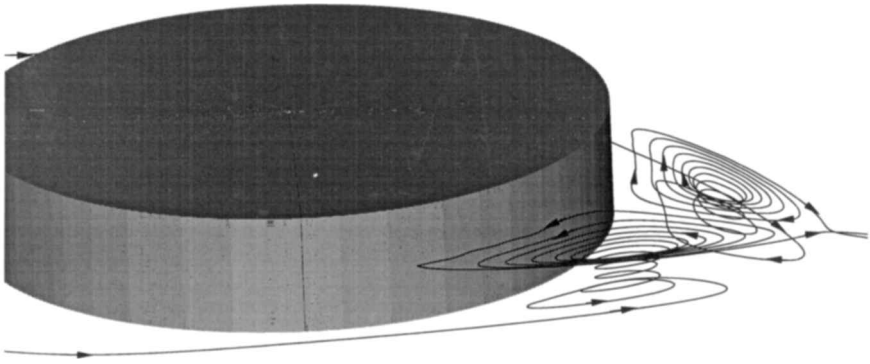

Figure 12. Illustration of the spiralling flow motion in the wake behind the cylinder tube.

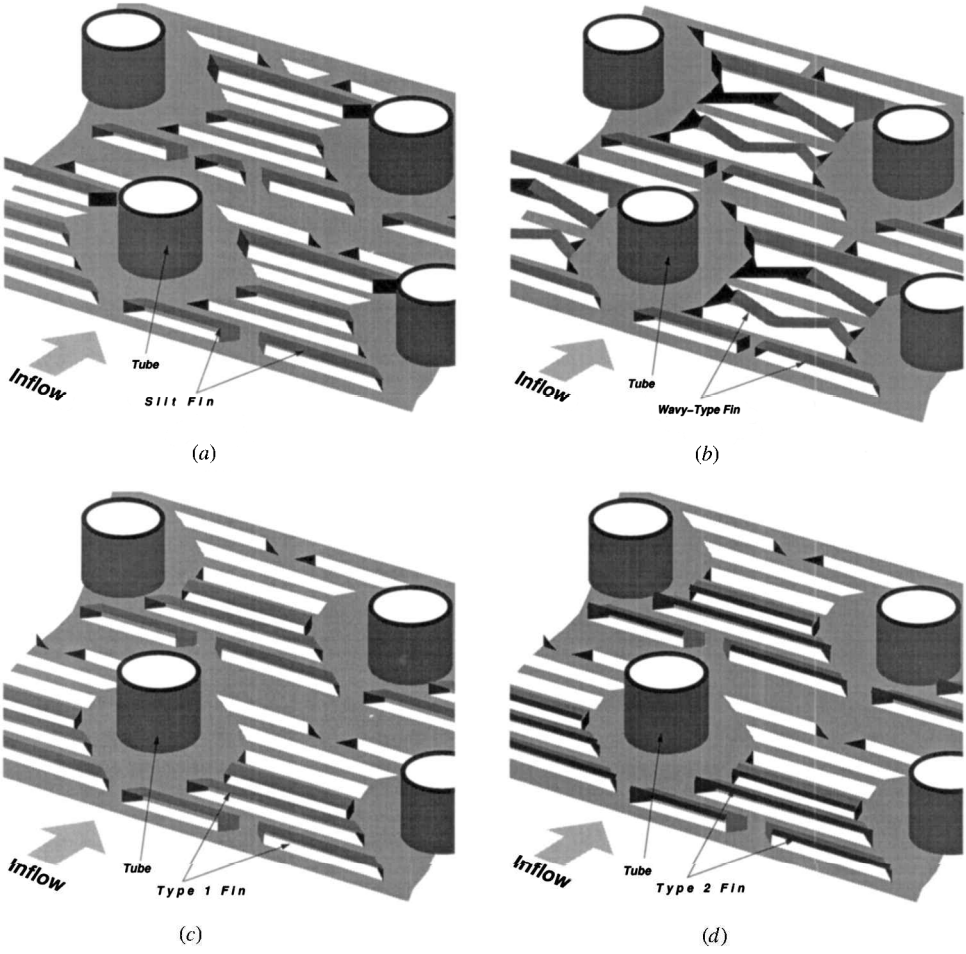

Figure 13. Schematic configurations of investigated fins: (*a*) slit type, (*b*) wavy type, (*c*) fin type 1, and (*d*) fin type 2.

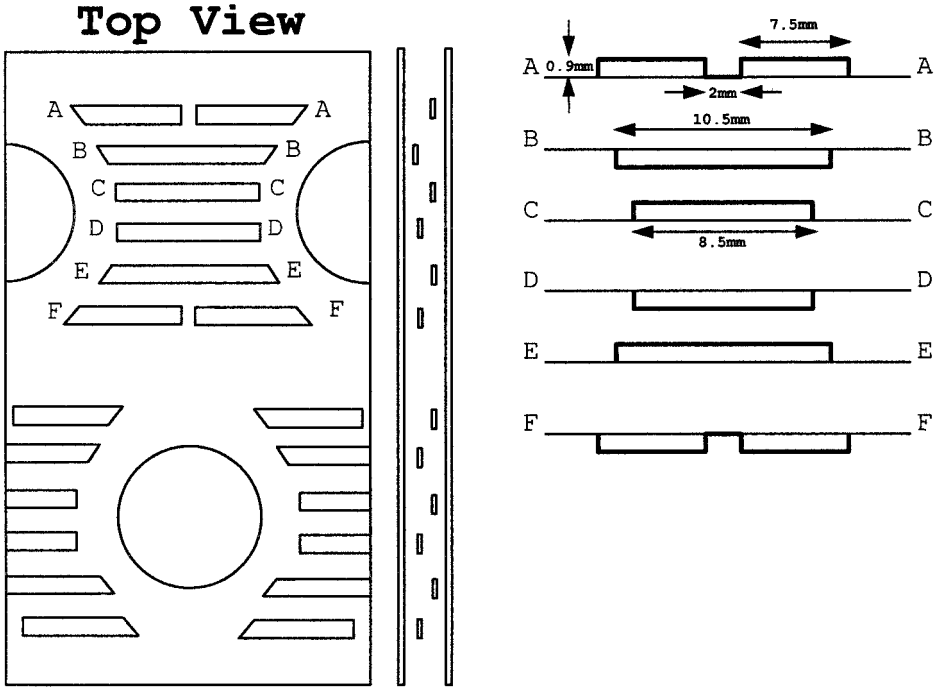

Figure 14. Top and side views of the investigated slit-type heat exchanger.

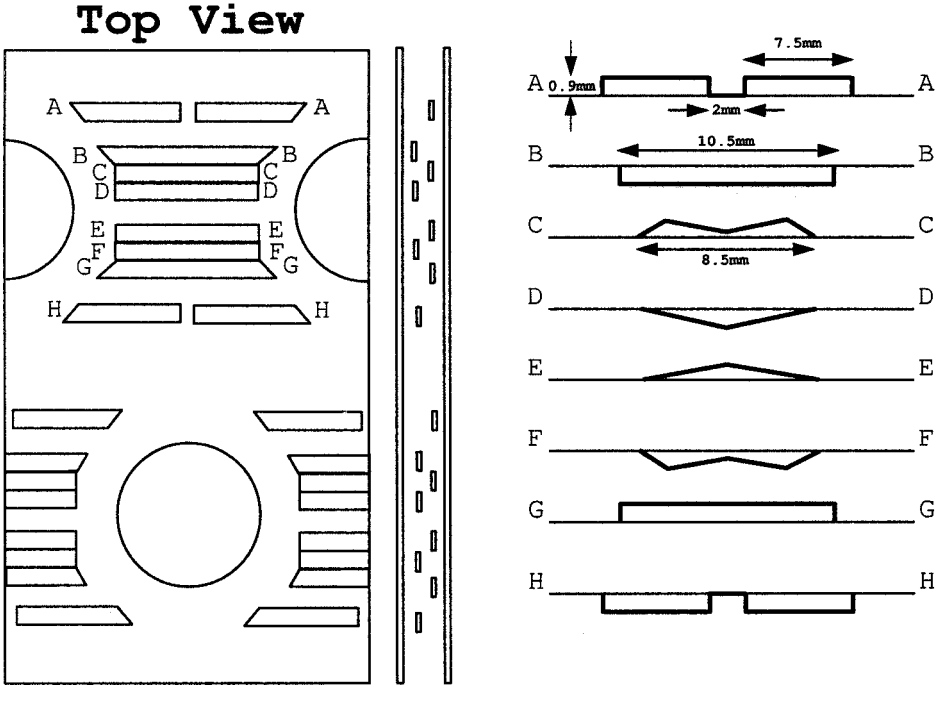

Figure 15. Top and side views of the investigated wavy-type heat exchanger.

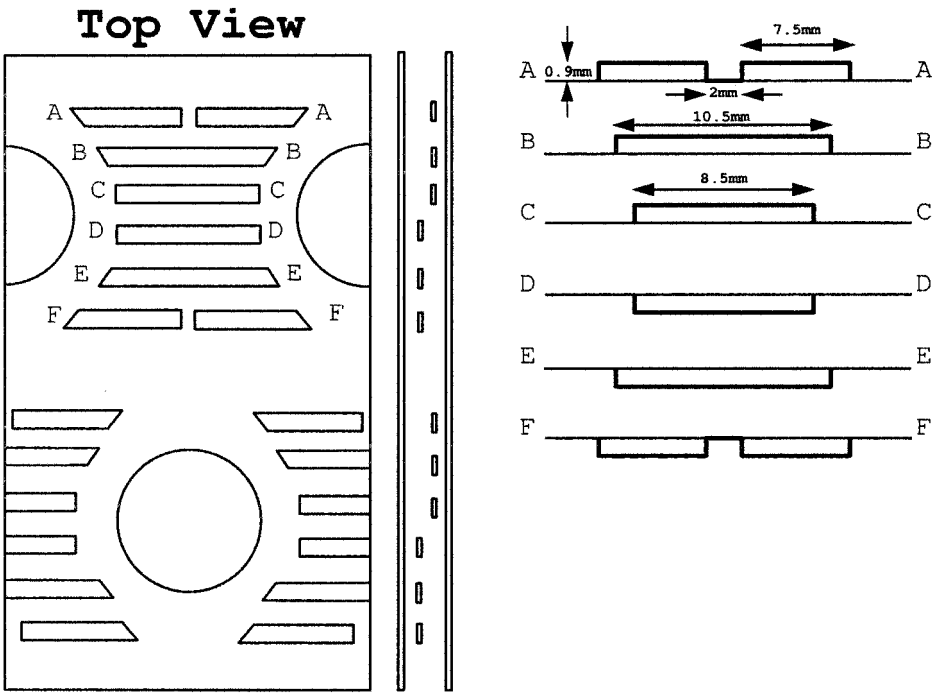

Figure 16. Top and side views of the other two investigated fins.

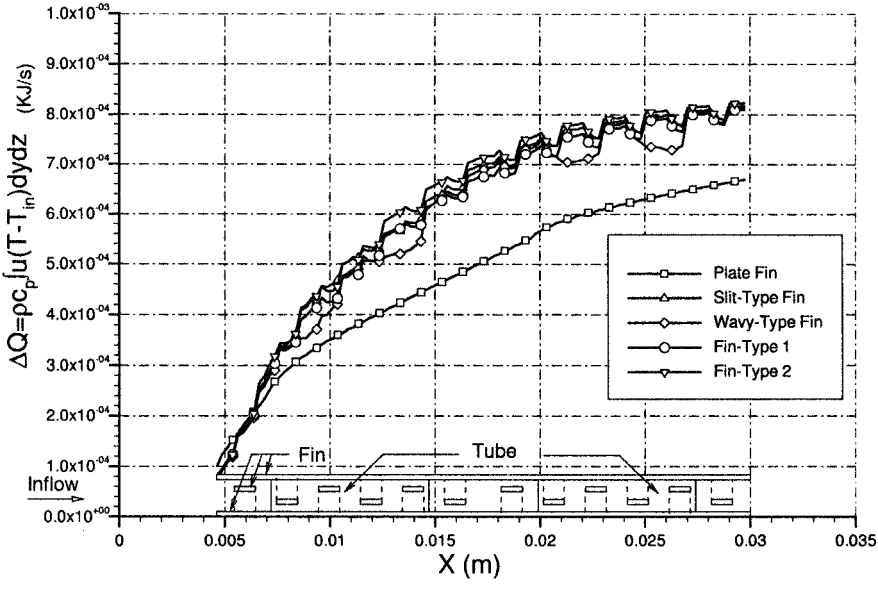

Figure 17. Span-averaged heat transfer in the streamwise direction for five investigated fin surfaces.

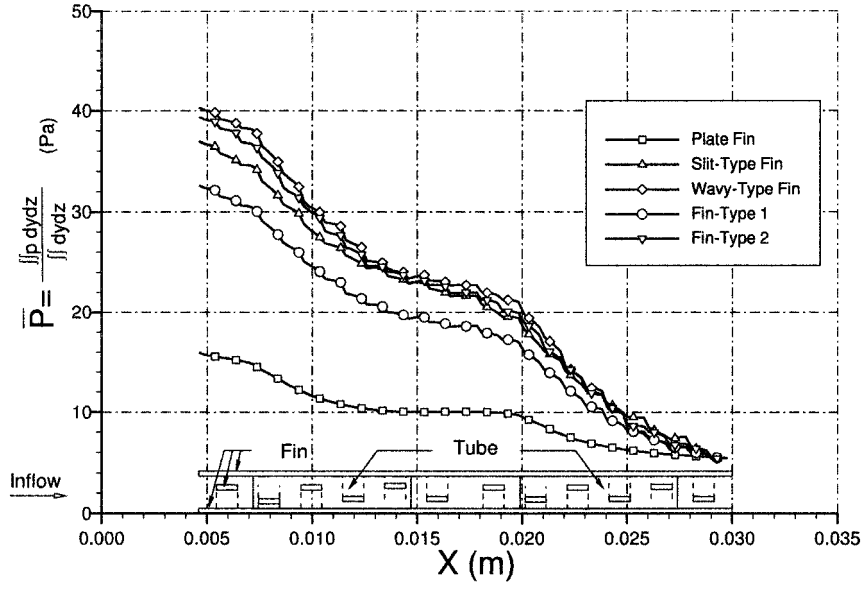

Figure 18. Averaged pressure distribution in the streamwise direction for five investigated fin surfaces.

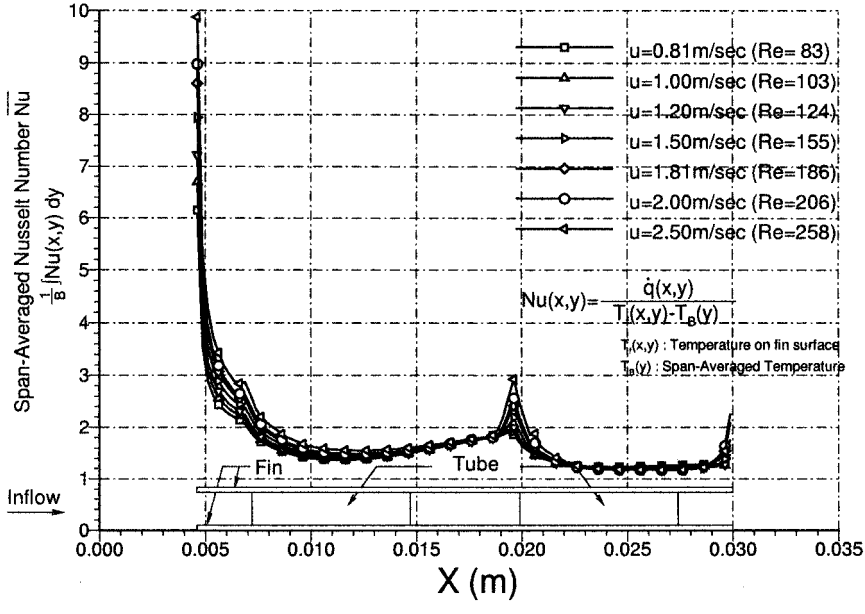

Figure 19. Span-averaged Nusselt numbers in the streamline direction as a function of Reynolds numbers for the plate fin under investigation.

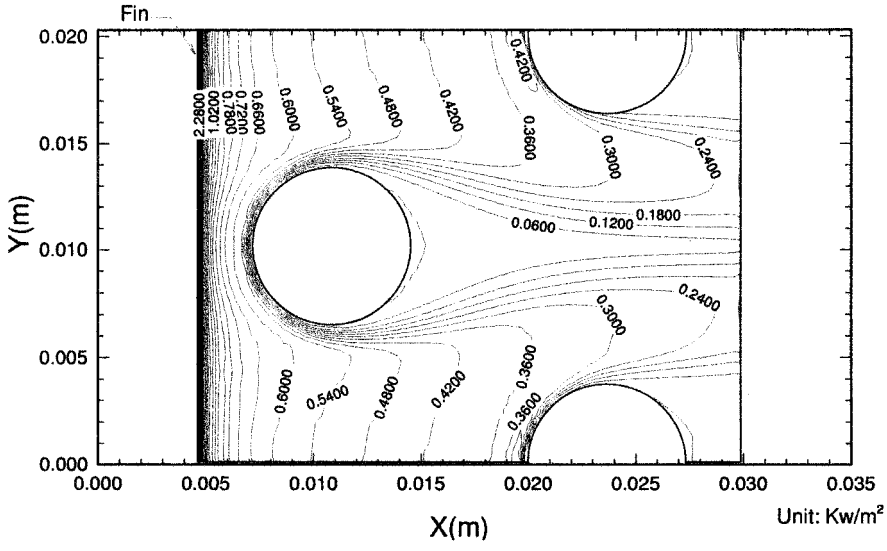

(*a*) plate fin

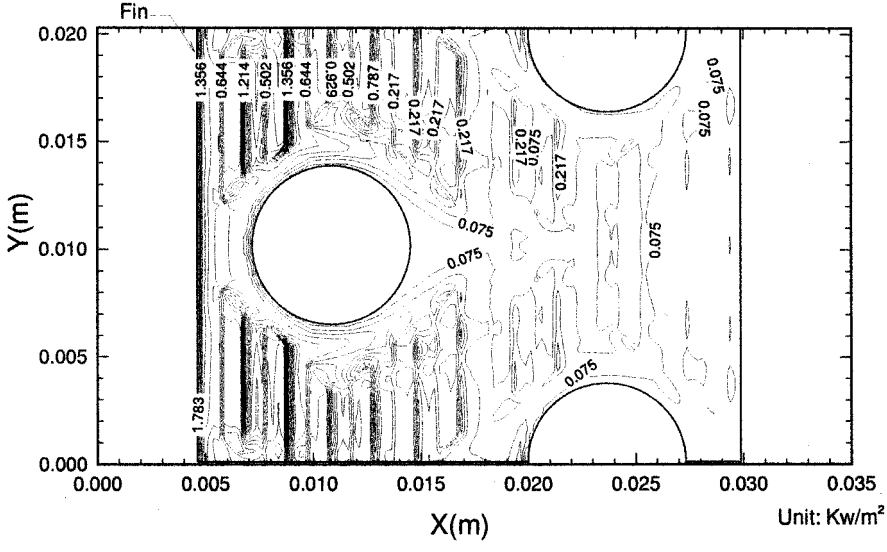

(*b*) slit type fin

Figure 20. Contour plots of heat flux $\dot{q}$ on different fin surfaces of heat exchanger.

nonuniform grids were invoked. The grid resolution is $142 \times 84 \times 54$ with $\Delta x_{\min} = 0.25$ mm, $\Delta y_{\min} = 0.25$ mm, and $\Delta z_{\min} = 0.014375$ mm. According to the obtained heat transfer capability, as shown in Figure 17, and the pressure drop, as shown in Figure 18, we are led to conclude that all the fins have increased heat transfer. Fin perforation also serves as a factor, aiding vortical flow formation, which can also

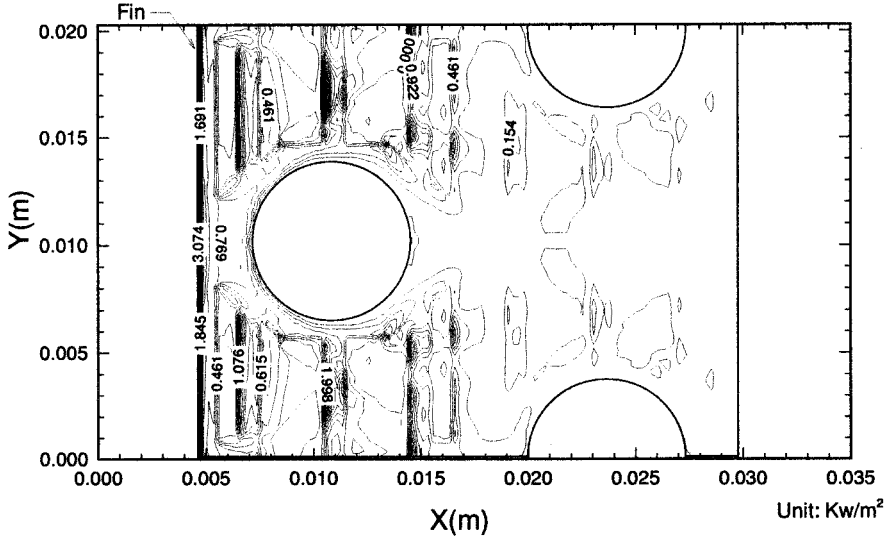

(*c*) wavy type fin

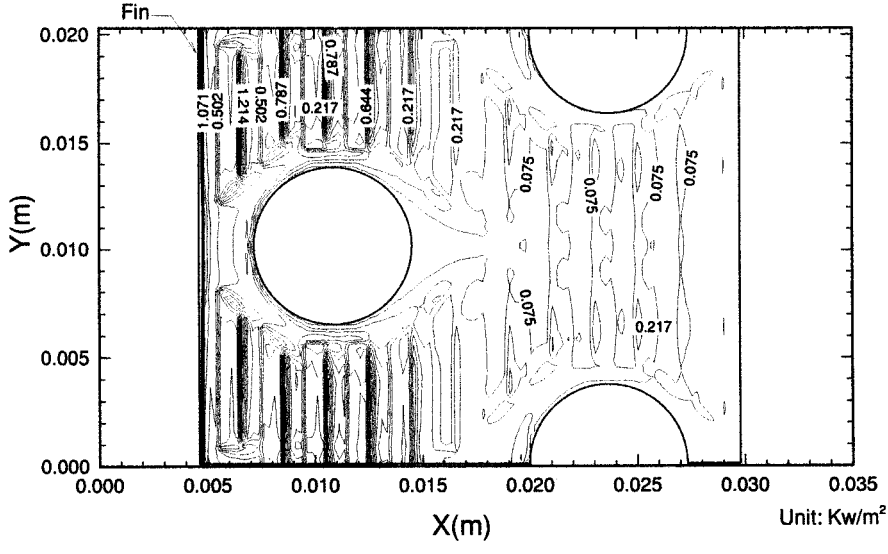

(*d*) Fin-type 1

Figure 20. Contour plots of heat flux $\dot{q}$ on different fin surfaces of heat exchanger (*Continued*).

enhance heat transfer between the fin surface and the surrounding airflow. As a result, it is clearly seen from Figure 17 that heat exchangers with slotted-fin surfaces outperform heat exchangers with plain surfaces. Among the slotted fins, heat transfer performance, as measured in terms of the span-averaged Nusselt

number, does not show too much difference (Figure 19). The vortical flow, which serves to enhance heat transfer, has, however, a negative effect on the pressure drop. The increase of the pressure drop can be seen clearly in Figure 18, which plots the streamwise averaged pressure at planes normal to the flow direction. For completeness, we also plot heat fluxes on the fin surface in Figure 20 in the contour-valued format. Based on the computed results shown in Figures 17–20, we suggest that fin type 1 has better performance.

CONCLUSION

A numerical investigation of laminar flow over two-row cylinder tubes has been presented for plate fins to validate the analysis code and for four slotted fins to assess their heat transfer performance. Based on the topological study of Legendre, the plotted streamlines in the flow interior and the limiting streamlines on the fin-tube surfaces help capture the finer details of the flow. Revealed by this study is the rich character of the obstacle-induced three-dimensional vortical flow, which is featured by the formation of a saddle point in front of the staggered cylinder, lines of separation and reattachment on the tube surface, and spiralling flow reversal in the wake of the cylinder. This study reveals that there is a trade-off between the benefit of having an improved heat transfer due to the fin perforation and the penalty of having to consume more power to account for the increased pressure drop.

REFERENCES

1. M. Fiebig, A. Grosse-Gorgemann, Y. Chen, and N. K. Mitra, Conjugate Heat Transfer of a Finned Tube, Part A: Heat Transfer Behavior and Occurrence of Heat Transfer Reversal, *Numer. Heat Transfer, Part A*, vol. 28, pp. 133–146, 1995.
2. M. Fiebig, Y. Chen, A. Grosse-Gorgemann, and N. K. Mitra, Conjugate Heat Transfer of a Finned Tube, Part B: Heat Transfer Augmentation and Avoidance of Heat Transfer Reversal by Longitudinal Vortex Generators, *Numer. Heat Transfer Part A*, vol. 28, pp. 147–155, 1995.
3. F. H. Harlow and J. E. Welch, Numerical Calculation of Time-Dependent Viscous Incompressible Flow of Fluid with Free Surface, *Phys. Fluids*, vol. 8, pp. 2182–2189, 1965.
4. B. P. Leonard, A Stable and Accurate Convective Modelling Procedure Based on Quadratic Upstream Interpolation, *Comput. Methods Appl. Mech. Eng.*, vol. 19, pp. 59–98, 1979.
5. L. A. Yates and G. T. Chapman, Streamlines, Vorticity Lines, and Vortices Around Three-Dimensional Bodies, *AIAA J.*, vol. 30, no. 7, pp. 1819–1825, 1992.
6. M. Tobak and D. J. Peake, Topology of Three-Dimensional Separated Flows, *Annul Rev. Fluid Mech.*, vol. 14, pp. 61–85, 1982.